Bioorganic & Medicinal Chemistry Letters 18 (2008) 4859–4863

Contents lists available at ScienceDirect

Bioorganic & Medicinal Chemistry Letters

journal homepage: www.elsevier.com/locate/bmcl

Discovery of 1,3-disubstituted-1*H*-pyrrole derivatives as potent Melanin-Concentrating Hormone Receptor 1 (MCH-R1) antagonists

Susanne Berglund [a], Bryan J. Egner [a], Henrik Gradén [a], Joakim Gradén [a], David G. A. Morgan [b], Tord Inghardt [a,*], Fabrizio Giordanetto [c,*]

[a] *Medicinal Chemistry, AstraZeneca R&D Mölndal, Pepparedsleden 1, SE-431 83, Mölndal, Sweden*
[b] *CVGI Bioscience, AstraZeneca R&D Alderley Park, Macclesfield, Cheshire SK 104TG, UK*
[c] *Lead Generation, AstraZeneca R&D Mölndal, Pepparedsleden 1, SE-431 83, Mölndal, Sweden*

ARTICLE INFO

Article history:
Received 16 June 2008
Revised 17 July 2008
Accepted 19 July 2008
Available online 24 July 2008

Keywords:
Melanin-Concentrating Hormone
MCH
MCH-R1 antagonists
Obesity

ABSTRACT

A series of 1,3-disubstituted-1*H*-pyrrole-based antagonists of the human Melanin-Concentrating Hormone Receptor 1 (h-MCH-R1) are reported. High-throughput screening of the AstraZeneca compound collection yielded **1,** a hit with moderate affinity towards MCH-R1. Subsequent structural manipulations and SAR analysis served to rationalize potency requirements, and **12** was identified as a novel, functional MCH-R1 antagonist with favorable pharmacokinetic properties.

© 2008 Elsevier Ltd. All rights reserved.

Worldwide obesity has been steadily increasing for the past 20 years.[1] In the United States, obesity is now the most common chronic disease, affecting one in three of all Americans, including children.[1] Morbidities associated with obesity and being overweight are contributing to more than 300,000 deaths per year among the US population, whereas the related economic expenditure has exceeded US $100 billions.[1]

The Melanin-Concentrating Hormone (MCH) system has attracted the interest of pharmaceutical companies due to its role in regulating food intake and energy expenditure in animal models. Specifically, it was shown that intracerebroventricular (icv) injection of MCH, a cyclic 19 amino acid peptide, promoted food intake in rats.[2] Additionally, mice overexpressing the MCH gene demonstrated hyperphagia and obesity traits,[3] while transgenic MCH Receptor 1 (MCH-R1) knockout mice displayed hyperactivity and a lean phenotype and were resistant to diet-induced obesity.[4] It was therefore postulated that MCH-R1 antagonism could offer a viable treatment for obesity and several MCH-R1 antagonists have been reported.[5–9] The discovery of novel, potent MCH-R1 antagonists with favorable in vivo pharmacokinetic properties is herein presented.

A high-throughput screening (HTS) campaign against MCH-R1 was initiated. It identified **1** (Fig. 1) as a hit with good receptor affinity (IC_{50} = 92 nM) but moderate functional antagonism (MCH-R1 GTPγS IC_{50} = 804 nM). Docking of **1** to a MCH-R1 homology model[10] postulated that the tertiary amine group and the carbonyl function engaged in polar interactions with the receptor, as shown in Figure 2. According to the docking, the 3,4-dichloro-benzyl group partially filled a narrow and extended hydrophobic pocket formed by the transmembrane helices 3, 5, and 6. Interestingly, these findings seem to be in agreement with a recently published structural model for MCH-R1 antagonism.[11] The nitro-thiophene fragment of **1** was considered problematic due to a number of concerns about metabolic stability and reactive metabolites formation. Chemical scan of an acid chlorides lead generation set was performed to identify appropriate structural replacements. Here, reagents were selected to ensure adequate coverage of chemical

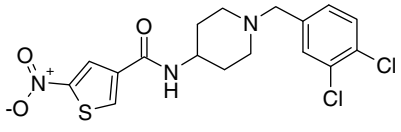

1 MCH-R1 IC_{50} = 0.092 μM
MCH-R1 GTPγS IC_{50} = 0.804 μM

Figure 1. Hit originated from in-house high-throughput screening campaign.

* Corresponding authors. Tel.: +46 31 7761954; fax: +46 31 7763724 (T. Inghardt), tel.: +46 31 7065723; fax: +46 31 7763710 (F. Giordanetto).
E-mail addresses: tord.inghardt@astrazeneca.com (T. Inghardt), fabrizio.giordanetto@astrazeneca.com (F. Giordanetto).

0960-894X/$ - see front matter © 2008 Elsevier Ltd. All rights reserved.
doi:10.1016/j.bmcl.2008.07.079

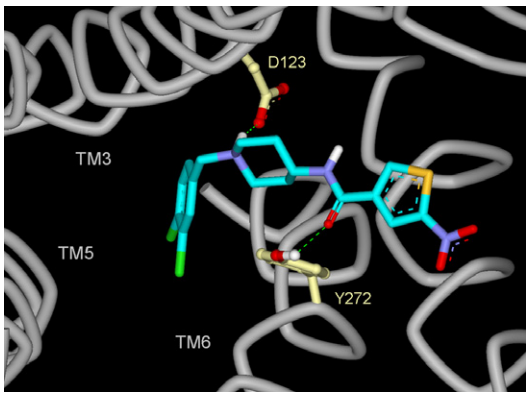

Figure 2. Predicted MCH-R1-docked conformation of **1**. Observed electrostatic interactions with D123 and Y272 side chains are displayed as dashed green lines.

space and, as a result, the 3-chloro-phenoxymethyl moiety was identified as a more suitable drug-like segment with similar MCH-R1 binding properties (MCH-R1 GTPγS IC_{50} = 1 μM) to the nitro-thiophene (MCH-R1 GTPγS IC_{50} = 0.8 μM), and it was used in the subsequent optimization efforts. Here, a number of elongated fragments were designed to validate the proposed structural framework and to investigate their effects on MCH-R1 potency. The results for derivatives **2**–**21** are presented in Table 1. The synthesis of **10** is reported in Scheme 1.[12]

Replacement of the phenyl ring in **1** with a lipophilic naphthalene (**2**) improved MCH-R1 potency and functional antagonism to 41 and 104 nM, respectively. On the contrary, the subsequent isosteric substitution of naphthalene to more polarized moieties, including 2,3-dihydro-benzo[1,4]dioxine (**3**), benzo[1,3]dioxole (**4**) and indole (**5**), was detrimental to affinity, as shown in Table 1. Inclusion of more extended biaryl fragments (**6**–**7**) failed to improve potency over **1** (Table 1). However, the introduction of 1-(4-

Table 1
In vitro MCH-R1 binding and functional data for **2**–**21**

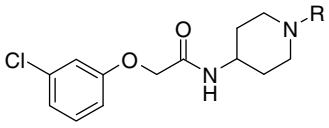

Compound	R	MCH-R1 IC_{50}[a] (GTPγS IC_{50})[b] (μM)	Compound	R	MCH-R1 IC_{50}[a] (GTPγS IC_{50})[b] (μM)
2	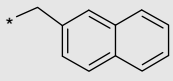	0.041 (0.104)	**12**	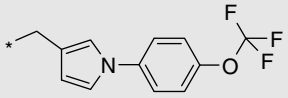	0.031 (0.015)
3	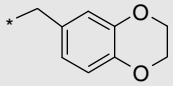	0.903	**13**	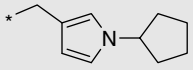	>33
4	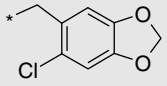	0.082 (0.505)	**14**	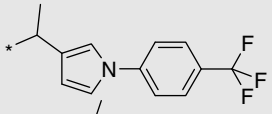	0.043 (0.117)
5	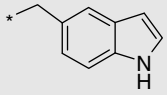	2.34	**15**	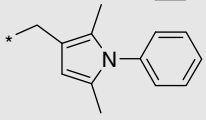	9.65
6	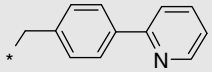	0.120	**16**	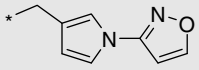	1.5
7	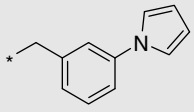	0.297	**17**	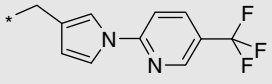	0.048 (0.092)
8	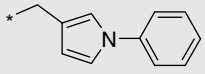	0.710	**18**	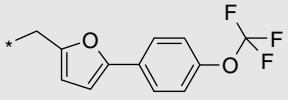	0.078 (0.103)
9	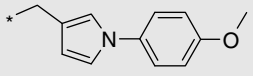	0.100 (0.090)	**19**	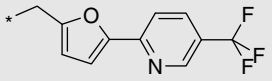	0.927
10	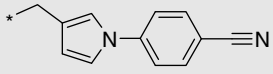	0.052 (0.145)	**20**	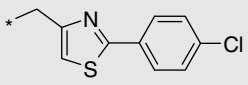	0.347
11	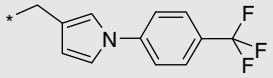	0.029 (0.032)	**21**	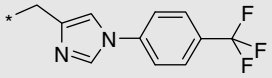	2.14

[a] Values are mean of at least two experiments. Compounds competed with ^{125}I-MCH for binding at the human MCH1 receptor (h-MCH-R1) expressed in the HEK293 cell line.
[b] Values are mean of at least two experiments. Functional assay measuring [^{35}S]GTPγS accumulation.

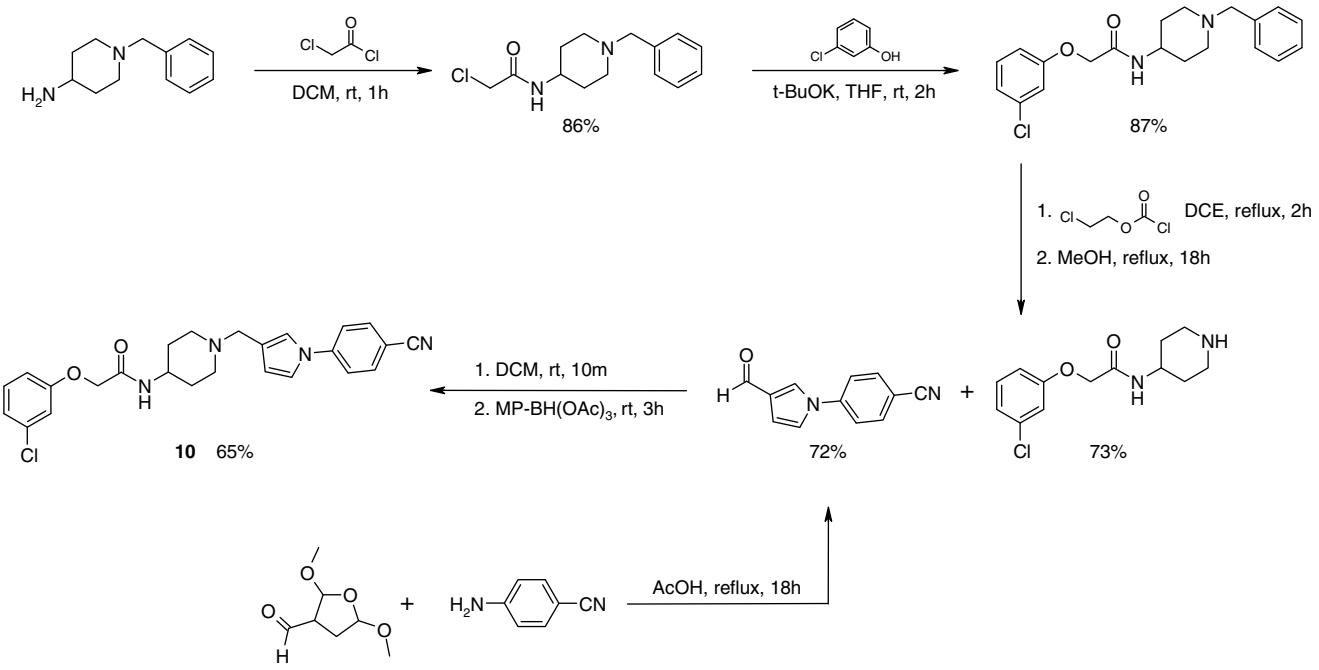

Scheme 1.

Table 2
In vitro MCH-R1 binding and functional data for **22**–**34**

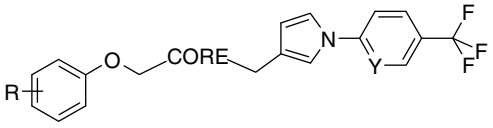

Compound	R	Core	Y	MCH-R1 IC_{50}[a] ($GTP\gamma S$ IC_{50})[b] (μM)	Compound	R	Core	Y	MCH-R1 IC_{50}[a] ($GTP\gamma S$ IC_{50})[b] (μM)
11	3-Cl	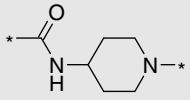	C	0.029 (0.044)	**28**	3,4-diF	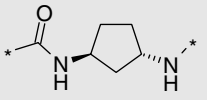	C	2.26
22	3-Cl	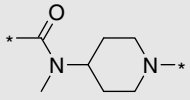	C	0.109	**29**	3,4-diF	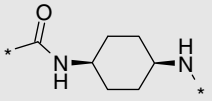	C	0.104
23	3-Cl	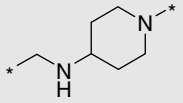	C	0.636	**30**	3-Cl	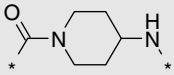	N	1.25
24	3-Cl	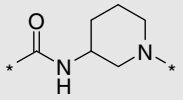	N	3.05	**31**	3-Cl	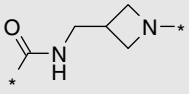	C	0.169
25	3,4-diF	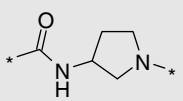	C	0.029 (0.048)	**32**	3-Cl	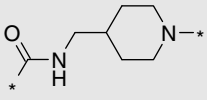	N	0.313
26	3-Cl	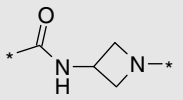	C	0.042 (0.073)	**33**	3-Cl	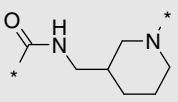	N	0.303
27	3-Cl	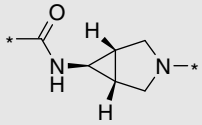	C	0.111	**34**	3,4-diF	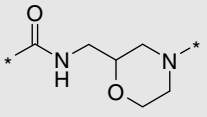	C	0.269

[a] Values are mean of at least two experiments. Compounds competed with ^{125}I-MCH for binding at the human MCH1 receptor (h-MCH-R1) expressed in the HEK293 cell line.
[b] Values are mean of at least two experiments. Functional assay measuring [^{35}S]GTPγS accumulation.

substituted-phenyl)-1H-pyrroles, **9**–**12**, afforded potent MCH-R1 antagonists. Here, electron-withdrawing groups seemed to be preferred over electron-donating substituents, probably reflecting the presence of electron rich tyrosines in the binding pocket. Specifically, the trifluoromethyl and trifluoromethyloxy groups provided the most potent, functional MCH-R1 antagonists (**11**: IC_{50} = 29 nM, GTPγS IC_{50} = 32 nM and **12**, IC_{50} = 31 nM, GTPγS IC_{50} = 15 nM, respectively). Branching on the pseudobenzylic position was tolerated, and afforded a potent MCH-R1 antagonist (**14**, IC_{50} = 43 nM) but no improvement in functional MCH-R1 antagonism (**14**, GTPγS IC_{50} = 117 nM). Additionally, increasing the steric bulk on the indole ring with a 1,5-dimethyl substitution resulted in a significant loss of MCH-R1 affinity (**15**, IC_{50} = 9.65 μM), thereby highlighting specific spatial constraints. Modification of the electronic properties of the distal ring had a significant effect on potency, as shown by the isoxazole (**16**, IC_{50} = 1.5 μM) and pyridine (**17**, IC_{50} = 48 nM) derivatives. Replacement of pyrrole with the 1,4-disubstituted furans, **18**–**19**, always translated in a potency loss. Similarly, the thiazole (**20**) and imidazole (**21**) counterparts failed to improve MCH-R1 potency, possibly validating the predicted lipophilic character of the MCH-R1 binding pocket.

The central part of the molecule was then subjected to extensive structural modifications in an effort to optimize MCH-R1 antagonism and to further explore the SAR around the present series. The results of such campaign are outlined in Table 2. Compounds **22**–**34** were prepared in a similar manner to Scheme 1, according to synthetic procedures previously disclosed.[12]

Direct manipulation of the amide function resulted in a diminished MCH-R1 affinity: the removal of the carbonyl group (**23**, IC_{50} = 636 nM) had a more evident effect than N-methylation (**22**, IC_{50} = 109 nM). This underlines the hypothesis of the involvement of the amide function in polar interactions with MCH-R1 (Fig. 2). Scaffold hopping to pyrrolidine (**25**) and azetidine (**26**) yielded potent MCH-R1 antagonists but no improvement in GTPγS IC_{50}, when compared to **11** or **12**. Fascinatingly, despite the obvious 2D and 3D similarities, introduction of 3-Aza-bicyclo[3.1.0]hex-6-ylamide (**27**) displayed a marked reduction in activity, which cannot simply be explained on the basis of ring flexibility alone. Modification of the interatomic distance between the amide and amine functions with 1,3-disubstituted cyclopentane (**28**) and cyclohexane (**29**) or when the 4-substituted-piperidine was flipped (**30**) did not improve MCH-R1 potency, as shown in Table 2. This is supported by the results obtained via one carbon chain homologation (**31**–**34**), affording IC_{50} values in the 169–313 nM range. Variation of the central scaffold indicated that there seem to be specific geometric constraints around the amide and amine groups of the present lead series. This might be due to the occurrence of electrostatic interactions with MCH-R1, which could be impaired by even the subtlest structural modifications, as exemplified by the data presented in Table 1. According to the emerging SAR, we concluded that a hydrogen bond acceptor (HBA) was beneficial to MCH-R1 potency, and we set to investigate alternative HBA functionalities, in the form of heterocycle fragments. The purpose was to retain the key HBA pharmacophore while reducing molecular flexibility, in order to lock the bioactive conformation of the compounds and improve their functional MCH-R1 antagonism. Compounds **35**–**40** were synthesized starting from commercially available building blocks, according to Scheme 2. Their MCH-R1 binding properties are outlined in Table 3.

Introduction of 5-substituted-imidazole, as a simple amide group bioisoster, afforded a compound (**35**) with good MCH-R1 potency (IC_{50} = 20 nM) but average functional activity (GTPγS IC_{50}: 122 nM). This indicates that while incorporation of a HBA feature via ring closure is tolerated in the binding pocket, there is no direct gain in efficacy. Interestingly, the 2-substituted-imidazole isomer **36** resulted in approximately sixfold potency loss, suggesting that

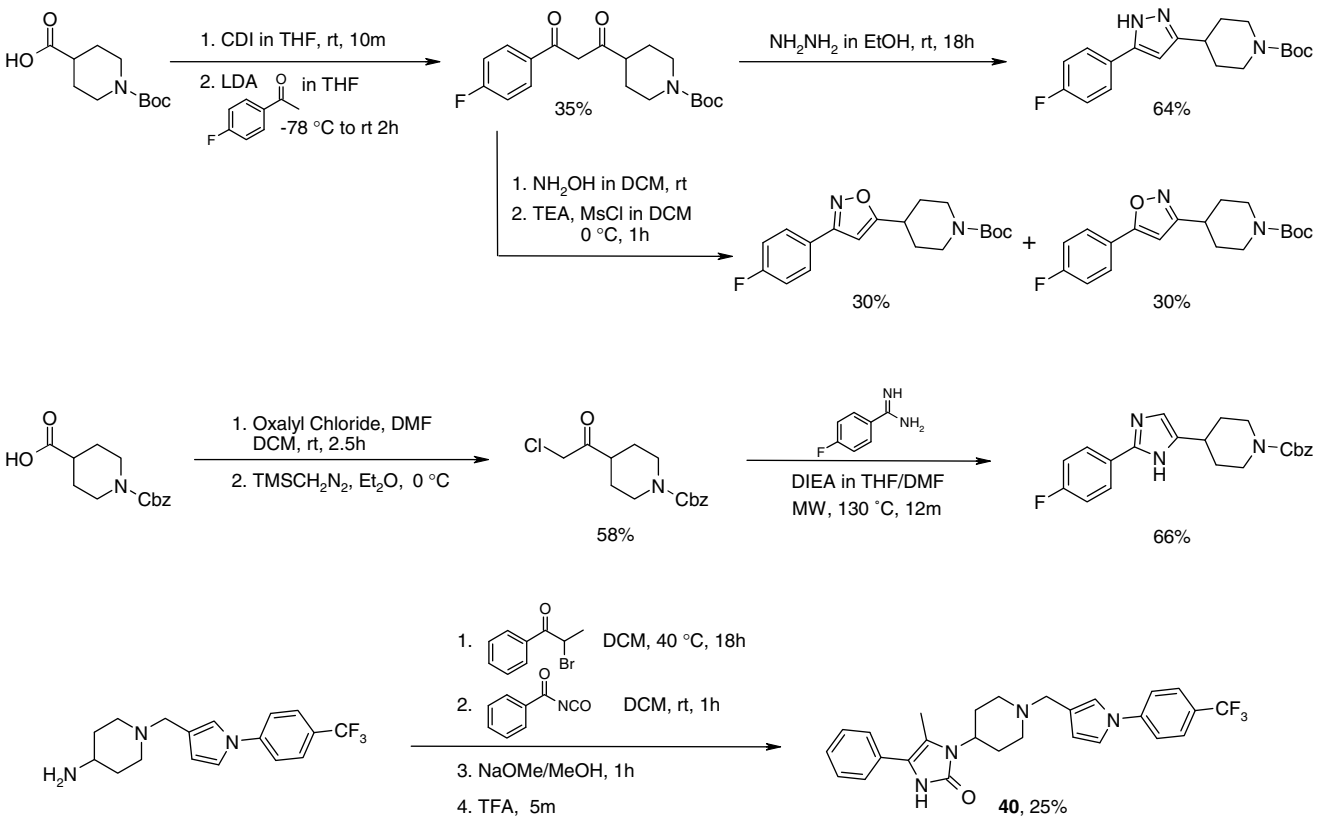

Scheme 2.

Table 3
In vitro MCH-R1 binding and functional data for **35**–**40**

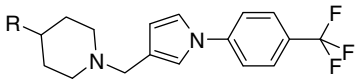

Compound	R	MCH-R1 IC_{50}[a] ($GTP\gamma S$ IC_{50})[b] (μM)	Compound	R	MCH-R1 IC_{50}[a] ($GTP\gamma S$ IC_{50})[b] (μM)
35	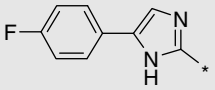	0.020 (0.122)	**38**	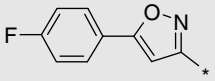	0.025 (0.067)
36	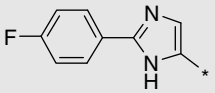	0.113	**39**	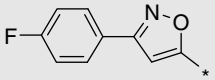	0.066
37	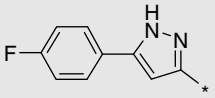	0.037 (0.058)	**40**	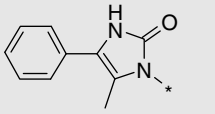	0.026 (0.071)

[a] Values are mean of at least two experiments. Compounds competed with ^{125}I-MCH for binding at the human MCH1 receptor (h-MCH-R1) expressed in the HEK293 cell line.
[b] Values are mean of at least two experiments. Functional assay measuring [^{35}S]$GTP\gamma S$ accumulation.

Table 4
Summary in vitro and in vivo data for **11** and **12**

	11	**12**
MCH-R1 $GTP\gamma S$ IC_{50}[a] (μM)	0.032	0.015
hERG IC_{50}[b] (μM)	0.56	0.49
F_u (% free)	1.2	3.2
HLM Cl_{int} (μL/min/mg)	38	21
Mouse Cl_{int} (iv)[c] (mL/min/kg)	41	34
Mouse $T_{1/2}$ (iv)[c] (h)	6	8.3
Mouse V_{ss} (iv)[c] (L/kg)	24	20
Mouse AUC (po) [c] (μM h)	11	1.2
Mouse $T_{1/2}$ (po) [c] (h)	10	14
Mouse bioavailability[c] (%)	100	100

[a] Functional assay measuring [^{35}S]$GTP\gamma S$ accumulation.
[b] Values are mean of at least two experiments. Patch clamp assay using IONWORKS™ technology in hERG-expressing CHO cells.
[c] Determined following oral administration of a 20 μM/kg nanosuspension dose in C57BL female mice.

the hydrogen bond interaction is indeed very susceptible to distance and directionality. This is supported by the data for the pyrazole (**37**) and isoxazole (**38**) derivatives, where the HBA atom is located in exactly the same position as in **35**. As a result, they displayed similar potency (IC_{50} = 37 and 25 nM, respectively) when compared to **35**, as shown in Table 3. Finally, cyclization of the amide functionality to provide the imidazol-2-one core resulted in a potent MCH-R1 antagonist (**40**, IC_{50} = 26 nM) but without the desired improvement in functional activity ($GTP\gamma S$ IC_{50} = 71 nM).

11 and **12** emerged as the most efficacious MCH-R1 antagonists in this study, displaying $GTP\gamma S$ IC_{50} values of 32 and 15 nM, respectively, as shown in Table 4. Moreover, the two compounds demonstrated acceptable free fractions in human plasma and appeared to be metabolically stable when tested in vitro in Human Liver Microsomes (HLM) preparations, as summarized in Table 4. Both **11** and **12** achieved high bioavailability following intravenous (iv) and oral (po) administration of a 20 μM/kg dose in mice (Table 4). Unfortunately, both derivatives were also found to be potent inhibitors of the hERG potassium channel, as outlined in Table 4, and this has represented a major hurdle for their subsequent development.

In summary, the optimization of the HTS hit **1** resulted in the discovery of 1-phenyl-1*H*-pyrrol-3-yl-derivatives as novel and potent MCH-R1 antagonists. Modification of the pyrrole and phenyl rings, as well as the central amine scaffold, indicated stringent electronic constraints in the MCH-R1 pocket. As a result of our structural exploration, **11** and **12** were shown to be functional MCH-R1 antagonists with favorable pharmacokinetic properties but intolerable cardiovascular safety margins. The subsequent hERG optimization efforts will be the subject of future publications from our group.

Acknowledgments

The authors thank their AstraZeneca R&D Mölndal colleagues Mia Boethius-Litzén for providing MCH-R1 binding and functional data as well as Lars-Olof Larsson and his team for providing the DMPK data. Clas Landersjö is greatly acknowledged for providing the structure elucidation by NMR of the isomeric isoxazoles.

References and notes

1. Melnikova, I.; Wages, D. *Nat. Drug Discov.* **2006**, *5*, 369.
2. Gomori, A.; Ishiara, A.; Ito, M.; Mashiko, S.; Matsuhita, H.; Yumoto, M.; Ito, M.; Tanaka, T.; Tokita, S.; Moriya, M.; Iwaasa, H.; Kanatani, A. *Am. J. Physiol. Endocrinol. Metab.* **2003**, *284*, E583.
3. Ludwig, D. S.; Tritos, N. A.; Mastaitis, J. W.; Kulkarni, R.; Kokkotou, E.; Elmiqst, J.; Lowell, B.; Flier, J. S.; Maratos-Flier, E. *J. Clin. Invest.* **2001**, *107*, 379.
4. Shimada, M.; Tritos, N. A.; Lowell, B. A.; Flier, J. S.; Maratos-Flier, E. *Nature* **1998**, *396*, 670.
5. Rivera, G.; Bocanegra-Garcia, V.; Galiano, S.; Cirauqui, N.; Ceras, J.; Perez, S.; Aldana, I.; Monge, A. *Curr. Med. Chem.* **2008**, *15*, 1025.
6. Kowalski, T. J.; Sasikumar, T. *Biodrugs* **2007**, *21*, 311.
7. Rokosz, L. L. *Exp. Opin. Drug Discov.* **2007**, *2*, 1301.
8. Souers, A. J.; Gao, J.; Brune, M.; Bush, E.; Wodka, D.; Vasudevan, A.; Judd, A. S.; Mulhern, M.; Brodjian, S.; Dayton, B.; Shapiro, R.; Hernandez, L. E.; Marsh, K. C.; Sham, H. L.; Collins, C. A.; Kym, P. R. *J. Med. Chem.* **2005**, *48*, 1318.
9. Takekawa, S.; Asami, A.; Ishihara, Y.; Terauchi, J.; Kato, K.; Shimomura, Y.; Mori, M.; Murakoshi, H.; Kato, K.; Suzuki, N.; Nishimura, O.; Fujino, M. *Eur. J. Pharmacol.* **2002**, *438*, 129.
10. Giordanetto, F.; Lindberg, J.; Karlsson, O.; Inghardt, T. Abstract of Papers, 232nd National Meeting of the American Chemical Society, San Francisco, CA, 2006, Abstract 0410.
11. Cavasotto, C. N.; Orry, A. J. W.; Murgolo, N. J.; Czarniecki, M. F.; Kocsi, S. A.; Hawes, B. E.; O'Neill, K. A.; Hine, H.; Burton, M. S.; Voigt, J. H.; Abagyan, R. A.; Bayne, M. L.; Monsma, M. J., Jr. *J. Med. Chem.* **2008**, *51*, 581.
12. The preparation of key compounds is described in: (a) Brickmann, K.; Egner, B. J.; Giordanetto F.; Inghardt, T.; Linusson, A.; Ponten, F. WO2005/090330 (Compounds **6–12, 17–18, 22, 25–26**) and in: (b) Egner, B. J.; Giordanetto, F.; Inghardt, T. WO2006/0685594 (Compounds **35–39**).